Materials Science in Semiconductor Processing 20 (2014) 68–73

Contents lists available at ScienceDirect

Materials Science in Semiconductor Processing

journal homepage: www.elsevier.com/locate/mssp

Photoacoustic study of optical and thermal properties of alloyed $CdTe_xS_{1-x}$ nanocrystals

Zahrah El-Qahtani [a], Ali Badawi [a,*], K. Easawi [b], N. Al-Hosiny [a,c], S. Abdallah [a,b]

[a] Department of Physics, Faculty of Science, Taif University, Taif 21974, Saudi Arabia
[b] Department of Mathematical and Physical Engineering, Faculty of Engineering (Shoubra), Benha University, Cairo, Egypt
[c] Department of Physics, Faculty of Science, Aljouf University, Aljouf, Saudi Arabia

ARTICLE INFO

Available online 29 January 2014

Keywords:
Alloyed $CdTe_xS_{1-x}$ nanocrystal
Photoacoustic spectroscopy
Thermal properties
Optical properties

ABSTRACT

Photoacoustic (PA) technique has been applied to study the optical and thermal properties of the alloyed $CdTe_xS_{1-x}$ (nanocrystals (NCs) with different (Te/(S+Te)) molar ratio (x=0, 0.2, 0.4, 0.6, 0.8 and 1). Increasing x value causes clearly observed red shift of the corresponding exciton peak in PA spectra. The same spectra were compared to those obtained by a regular UV–Vis. absorption. The effective mass approximation (EMA) model was applied to determine the size of the NCs. The calculated sizes of the alloyed NCs are in a good agreement with the directly measured values obtained using high resolution transmission electron microscopy (HRTEM). The values of thermal diffusivity and thermal conductivity obtained using PA technique show at least an order of magnitude larger than that of the bulk values.

1. Introduction

In the last few decades, the main efforts have been focused on II–VI (CdSe, CdTe, ZnSe and CdS) semiconductor nanocrystals (NCs), due to their unique size-dependent optical and thermal properties [1–4]. However, tuning their properties by changing the particle size may causes problems in some applications, in particular, if unstable small particles (less than 2 nm) are used. This is because very small NCs with a short emission wavelength remain very different to passivate and exhibit unstable optical properties [5]. To overcome these problems, a new class of alloyed semiconductor NCs have been studied [5,6] to provide a way for continuous tuning of their energy band gap without changing the particle size. Semiconductor alloyed NCs (AB_xC_{1-x}) [7,8] are becoming increasingly important in many areas of nanoscale engineering because of the continuous tunability of their physical and optical properties through gradual variation of the composition variable x. Owing to their superior luminescent properties that are on par with binary NCs ternary alloys are now well suited for many practical realizations, including quantum dot-based LEDs [9], where emission at a specific wavelength is often required; in vivo imaging [8,10], where small diameter infrared fluorescence labels are preferred; and solar cells [4,11–13], where a wide range of absorption and the small size of NCs sensitizers are required. The band gap of $CdTe_xS_{1-x}$ alloyed NCs can be adjusted by varying the tellurium molar ratio, spanning the compositional range from pure CdS (x=0) to pure CdTe (x=1), where the band gap energies ranges from the UV to Near Infra Red region. This makes $CdTe_xS_{1-x}$ NCs a potentially favorable material for photovoltaic solar cell applications, where NCs of the same size but with varying optical properties might be advantageous. Measurement of thermal parameters such as thermal diffusivity (α), thermal effusivity (e) and thermal conductivity (k) for alloyed NCs are very essential for their applications, particularly in the fabrication of solar cells. α(m^2/s) is a significant thermo physical parameter which measures how effectively

* Corresponding author. Tel.: +966543414808; fax: +96627241880.
E-mail address: adaraghmeh@yahoo.com (A. Badawi).

1369-8001/$ - see front matter © 2014 Elsevier Ltd. All rights reserved.
http://dx.doi.org/10.1016/j.mssp.2013.12.034

phonons carry heat through the sample. Whereas the measurement of the heat exchange rate or the thermal impedance for heat exchange of a given material is essentially determined by e ($W\,s^{1/2}/m^2/K$). e is a relevant thermo physical parameter for surface heating or cooling processes as well as in quenching processes. These quantities are defined by $\alpha=k/\rho c$ and $e=\sqrt{k\rho c}$, where c is the specific heat capacity and ρ is the mass density. Knowing α, and e, the sample thermal conductivity can be obtained from the relation $k=e\sqrt{\alpha}$.

Photoacoustic technique (PA) is a photothermal (PT) detection technique; that is proved to be a powerful tool to study the optical, electronic, and thermal properties of such material in a nondestructive manner without particular sample treatment [1,14–16]. The sample to be studied is placed inside a gas/microphone cell, in which a portion of thermal energy is produced in the sample by light absorption. Subsequent thermalization within the sample produce a pressure fluctuation in the air within the cell which is detected as an acoustic signal by a sensitive microphone attached to the cell. Therefore, the PA signal contains information about the optical absorption within the sample in addition to the way with which the heat is diffused through the sample [14]. The applications of the PA technique have been efficiently extended to liquids and solids only after the successful formulation of a general theoretical model by Rosencwaig and Gersho in mid-seventies [16–20]. Subsequent developments in the theoretical aspects of PT phenomena are mere extensions or modifications of Rosencwaig–Gersho model [16].

In the present work, we study the dependence of PA spectra for alloyed $CdTe_xS_{1-x}$ NCs on the varying the tellurium molar ratio ($x=0$ to 1) to investigate the effect of molar ratio on the band gap for alloyed $CdTe_xS_{1-x}$ NCs. The PA spectra were also confirmed by UV–Vis. spectra technique. Vegard's law was applied to obtain the band gap of bulk alloyed $CdTe_xS_{1-x}$ (E_g bulk). The nanocomposite size was calculated using the exciton energy and the effective mass approximation (EMA) model. The obtained particles sizes were compared to that measured by high resolution transmission electron microscope (HRTEM). Furthermore, PA technique was used to determine the values of α, e and k of the alloyed $CdTe_xS_{1-x}$ NCs of different molar ratio x.

2. Experiment

A series of alloyed $CdTe_xS_{1-x}$ NCs samples ($x=0$, 0.2, 0.4, 0.5, 0.6, 0.8, and 1.0) were synthesized as the method of Talapin et al. [21] by varying the amount of the second precursor. Cadmium solution was prepared by 0.3 g of CdO added to 3.0 g of stearic acid, and heated up to 170 °C till the red color of CdO disappears to ensure that the reaction between CdO and stearic acid is complete and CdO completely transform to Cd sterate. 2.0 g of tri-*n*-octylphosphine oxide (TOPO) and 1.0 g of hexadecyleamine (HDA) were added to the reaction mixture and heated at 200 °C. For example in the preparation of $CdTe_{0.4}S_{0.6}$ NCs sample, Tellurium solution was prepared by mixing 0.53 g of tellurium in 1.5 mL of trioctylphosphine (TOP). Sulfur solution was also prepared by dissolving 0.2 g of sulphur in 1.5 mL of TOP. The mixture was then injected into the cadmium solution at 200 °C. Appropriate amounts of sulfur and tellurium solutions were mixed together to give the above ratios. Six samples with different molar ratios ($x=0$, 0.2, 0.4, 0.6, 0.8, and 1) were obtained from the reaction mixture at time interval of 7 min. For PA measurements, samples in the powder nature were compressed under a hydraulic pressure of 1 t/cm^2 to form pellets. They were labeled from *a* to *f* according to increasing the value of *x*.

PA measurements were carried out by a gas microphone technique. The light beam from tungsten-halogen lamp (1000 W) (New-port model 66885) was focused into the entrance slit of a monochrometer (Newport oriel product line model 74125). The output beam of the exit slit was mechanically modulated by a mechanical chopper (SR540), and focused onto the sample which was mounted carefully inside a PA cell (MTEC Model 300). The sound wave generated from the sample can be subsequently detected as an acoustic signal by a highly sensitive electrical microphone fixed in the PA cell. The PA signal was then amplified by a low noise preamplifier and further processed using a lock-in amplifier (Stanford Research System, Model SR830 DSP). A personal computer was interfaced to the system for automatic data acquisition and analysis. Measurements of PA spectra were carried out at room temperature in the wavelength range 375–675 nm at modulation frequency 15 Hz using a mechanical chopper. The PA spectra were normalized (light intensity normalization) using carbon black sample in the allowed region of the used tungsten-halogen lamp. Fig. 1 shows the schematic diagram of the PA experimental set-up for optical absorption (energy band gap) measurements of the alloyed $CdTe_xS_{1-x}$ NCs samples [1,15].

For thermal properties measurements, the same set-up was used but the tungsten-halogen light source and the monochrometer was replaced by 200 mW (514 nm) argon ion laser (Melles Griot, Carlsbad, CA 92009).

3. Results and discussion

3.1. Particle size determination

The average particle size distributions of the samples were measured using HRTEM (JEOL 311UHR operated at 300KV). Specimens were prepared by depositing a drop of hexane solution onto a Formvar-coated copper grid and letting it to dry in air. Fig. 2(a) and (b) shows the HRTEM

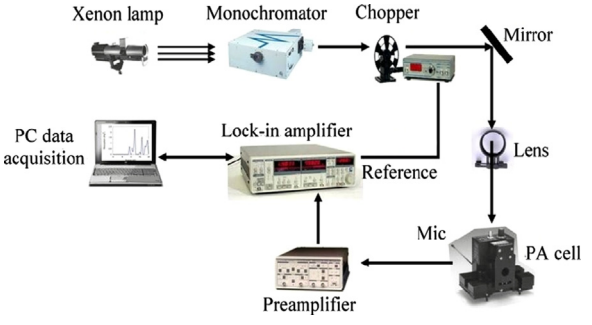

Fig. 1. The schematic diagram of the PA experimental set-up for optical absorption measurements.

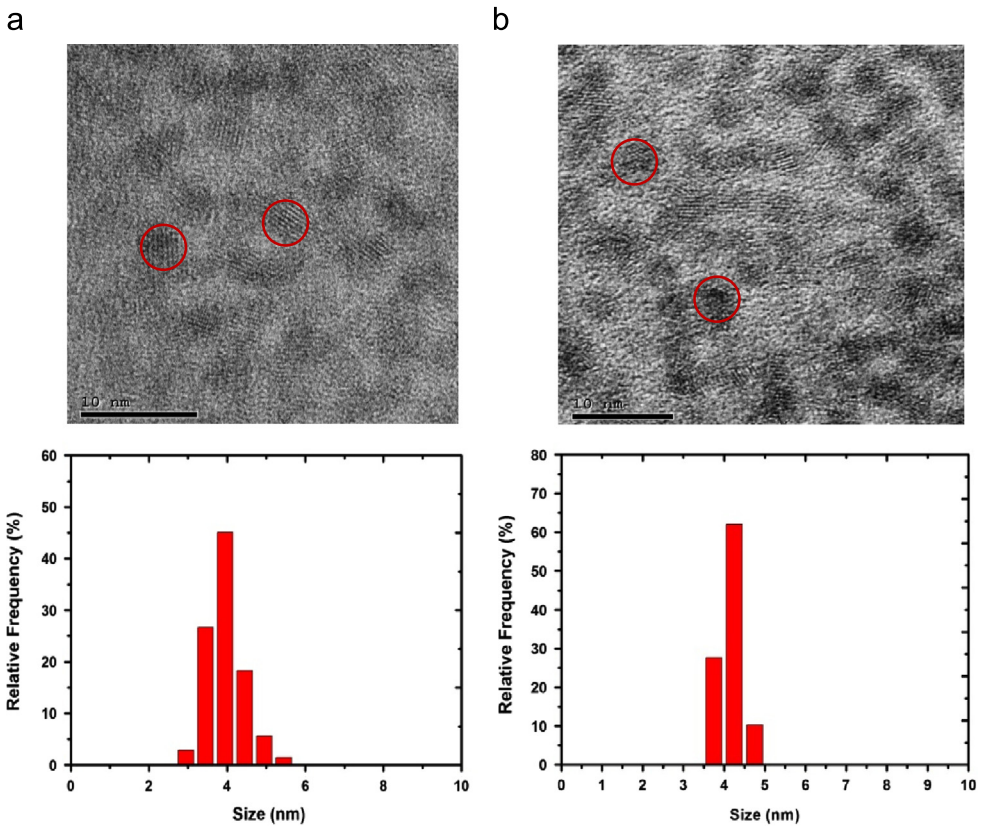

Fig. 2. HRTEM images and the corresponding histogram for $CdTe_xS_{1-x}$ for: (a) $x=0.2$ and (b) $x=0.8$.

micrographs for alloyed $CdTe_xS_{1-x}$ NCs and their corresponding histogram for $x=0.2$, and 0.8 respectively as examples. The sizes of alloyed NCs are: 3.9, 3.95, 4.02, 3.85, 4.1, and 4.0 nm for $x=0$, 0.2, 0.4, 0.6, 0.8, and 1, respectively. It is observed that the particles sizes of all samples are approximately equal (3.97 ± 0.30 nm). Ultra-high resolution images of the 10 nm nanoparticles are showing the crystal lattice planes.

3.2. Optical absorption measurements

For PA spectroscopy measurements, alloyed NC sample as a powder form was compressed under a hydraulic pressure of 1 t/cm^2 into disks of a diameter of 1 cm and a thickness of 1.65 ± 0.05 mm for each. While for UV–Vis. measurements, a colloidal solution of each alloyed NC sample was also prepared. The PA signal amplitude was recorded at chopping frequencies (f) varies from 4 to 200 Hz for each sample. Fig. 3(a) shows the PA spectra for the six investigated samples of alloyed $CdTe_xS_{1-x}$ NCs (a–f) as a function of the wavelength of the incident beam (from 375 to 675 nm). For the indicated tellurium to sulfur ratio, the absorption spectra show a single edge varying from 427 nm for $x=0$ to 611 nm for $x=1$. This behavior indicates that the samples are truly alloyed. The calculated energy band ($E=hc/\lambda$) for the same samples varies from 2.90 eV for $x=0$ to 2.00 eV for $x=1$. The optical absorption spectra of the same samples in colloidal solution were also obtained by regular UV–Vis. spectrophotometer and given in Fig. 3(b). It is easily observed that, the absorption edge varies from 431 nm for $x=0$ to 605 nm for $x=1$. The corresponding energy gaps are 2.87 and 2.04 eV, respectively. Although, the UV–Vis. spectra are for samples in colloidal form, and the PA spectra are for powder form, the two spectra gave peaks that are very close. The slight difference in the absorption edges positions of alloyed $CdTe_xS_{1-x}$ NCs between PA and UV–Vis. spectra may be due to the difference in characteristics of the acoustic wave in PA (non-radiative nature signal) and the photonic character of the UV–Vis. The red-shift of the PA and UV–Vis. absorption spectra of the alloyed $CdTe_xS_{1-x}$ NCs with increasing Te content is due to the decrease of the band gap caused by the incorporation of Te (as shown in Fig. 3). Meanwhile, the sharp absorption feature suggests highly monodisperse distribution. Furthermore, the PA technique is able to give the absorption spectra of as prepared semiconductor nanoparticles of different ratio more resolved than the UV–Vis absorption spectrum.

In order to calculate the particle size of alloyed $CdTe_xS_{1-x}$ NCs, we have employed Vegards law [8,22] first to calculate the band gap of alloy bulk, and then we use the effective mass approximation (EMA) model to get the particle size which is given by Refs. [4,23–27].

$$E_g(\mathrm{NC}) = E_g(\mathrm{bulk}) + \frac{h^2}{8R^2}\left[\frac{1}{m_e}+\frac{1}{m_h}\right] - \frac{1.8e^2}{4\pi\varepsilon\varepsilon_0 R} \quad (1)$$

where E_g(NC) is the lowest energy of electronic transition for NCs, E_g(bulk) is the band gap of bulk material, R is

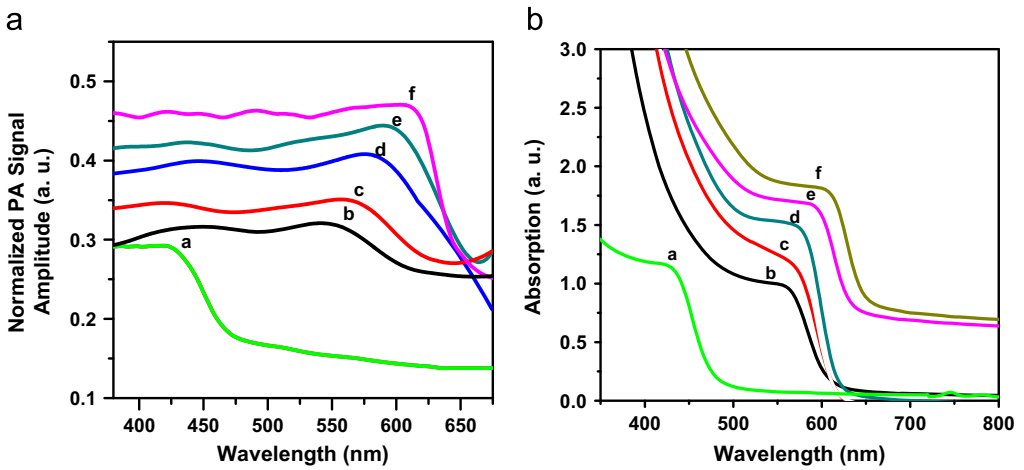

Fig. 3. (a) Normalized PA spectra, and (b) UV–Vis absorption spectra for alloyed $CdTe_xS_{1-x}$ NCs (*a–f*).

Table 1
The band gaps, reduced masses, dielectric constants and the particle size obtained from PA spectra and HRTEM.

x	E_g (bulk) (eV)	E_g (NC) (eV)	Reduced mass 10^{-31} kg	ε	Particle size (± 0.2 nm) by PA	Particle size (± 0.3 nm) by HRTEM
0	2.42	2.90	1.3	5.29	3.82	3.9
0.2	1.73	2.22	1.29	5.652	3.83	3.9
0.4	1.29	2.19	1.16	6.014	3.79	4.0
0.6	1.106	2.11	1.02	6.376	3.91	3.8
0.8	1.164	2.07	0.89	6.738	3.83	4.1
1	1.47	2.00	0.75	7.1	3.92	4.0

particle radius, m_e (0.11 m_0 for CdTe and 0.7 m_0 for CdS) [28] and m_h (0.35 m_0 for CdTe and 0.2 m_0 for CdS) are the effective mass of electron and hole, respectively, where m_0 is the free mass of electron, ε (=7.1 for CdTe and 5.29 for CdS) [28] is the relative dielectric constant, ε_0 is the vacuum permittivity, and e is the electron charge. The energy gap of the alloy can be obtained using Vegard's law as follows [8,22]

$$\chi(CdTe_xS_{1-x}) = x\chi(CdTe) + (1-x)\chi(CdS) - x(1-x)b \quad (2)$$

where χ stands for E_g (bulk) for CdTe (=1.47 eV) and for CdS (=2.42 eV [28], x is the Te mole fraction, and b is the bowing parameter=3.17 [7] for $CdTe_xS_{1-x}$ alloy. The corresponding values of m_e, m_h and ε for the alloyed NCs were also obtained in the manner above. Table 1 shows the calculated values of constants E_g (bulk), m_e, m_h, and ε for the bulk alloyed $CdTe_xS_{1-x}$.

As can be seen from Table 1, the energy gap for all value of x of alloyed $CdTe_xS_{1-x}$ NCs are shifted to higher energy with respect to their corresponding bulk values. Such blue shifts with respect to bulk alloyed $CdTe_xS_{1-x}$ are considered due to excellent quantum confinement effect. Furthermore, it is observed that the calculated particle sizes using PA spectra of alloyed NCs for each composite x are in good agreement with the measured one by HRTEM. Therefore the use of Vegard's law is fundamental to get alloy NCs parameters.

3.3. Thermal parameter measurements

The PA technique was also employed to investigate the thermal properties of the alloyed $CdTe_xS_{1-x}$ NCs. The powder of each sample was compressed (under hydraulic pressure of 1 t/cm^2) into a disk as mentioned before. The PA signal amplitude was recorded at various chopping frequencies (f) for each sample (depth profile analysis). The plots of ln PA amplitude versus the ln (f) for alloyed NCs samples are shown in Fig. 4(a) and (b) for $x=0.2$ and $x=0.8$, respectively. The distinct change in slope, at the characteristic frequency (f_c) where the crossover take place can be easily observed. f_c is the modulation frequency at which the sample changes from being thermally thick ($\mu_s > L$) to thermally thin ($\mu_s < L$), where μ_s is the sample thermal diffusion length and L is the sample's thickness. The thermal diffusivity (α) was then calculated using the relation [1,29]

$$\alpha = f_c L^2 \quad (3)$$

The values of α are calculated and given in Table 2 for the alloyed NCs samples of different molar ratios.

The thermal effusivity (e) of the samples was also determined by PA technique, where for optically opaque and thermally thick sample, the PA signal amplitude q is given by Ref. [1,15,30].

$$q = \frac{B}{e}\frac{1}{f} \quad (4)$$

where $B = (I_0/2)(\gamma P_0 \alpha_g^{1/2}/2\pi l_g T_0)$, I_0 is the incident light intensity, γ is the ratio of specific heats, P_0 is the ambient pressure, α_g is the gas thermal diffusivity, l_g is the length of the gas column, T_0 is the ambient temperature and f is the modulation frequency. Using Si as a reference sample, with thermal effusivity given by 15,670 W s$^{1/2}$/m^2/K [1]. The reference Si sample is used to eliminate the constant factor B by normalizing the signal measured for the sample to that measured for Si. The e values obtained for different samples are given in Table 2. Where the slopes of the both the Si and the sample were obtained from Fig. 5 by linear fitting for the relation between ($1/f$) and PA amplitude (q).

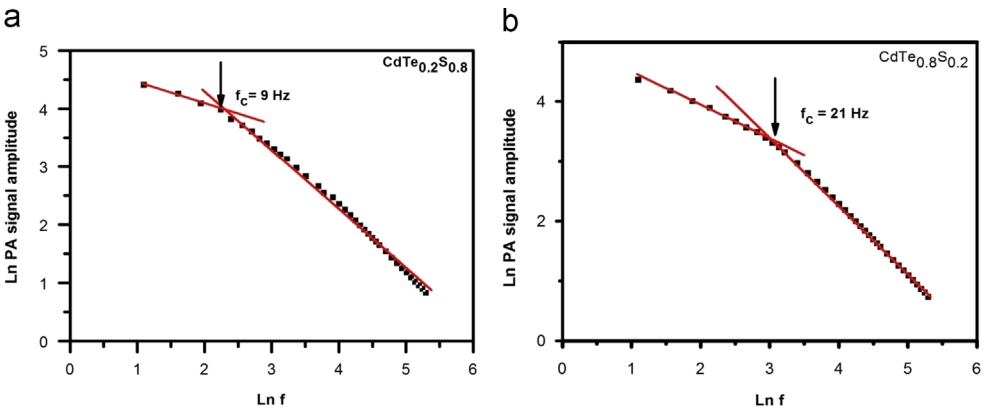

Fig. 4. Variation of ln PA signal amplitude versus ln f for alloyed $CdTe_xS_{1-x}$ NCs at: (a) $x=0.2$ and (b) $x=0.8$.

Table 2
Thermal parameters of alloyed $CdTe_xS_{1-x}$ NCs.

x	Thermal diffusivity (α) (10^{-5} m^2/s) $\pm$ 0.05	Thermal effusivity (e) (W $s^{1/2}/m^2/K$) $\pm$ 7	Thermal conductivity (k) (W/m K) $\pm$ 0.5
0	2.52	4,300	21.5
0.2	2.61	4,314	22.0
0.4	3.25	7,071	45.6
0.6	4.31	10,217	67.6
0.8	5.46	10,886	80.4
1	6.52	12,087	97.4
Bulk CdTe	0.59 [21]	3,705	9 [25,26]
Bulk CdS	0.03 [21]	1,300	0.79 [21]

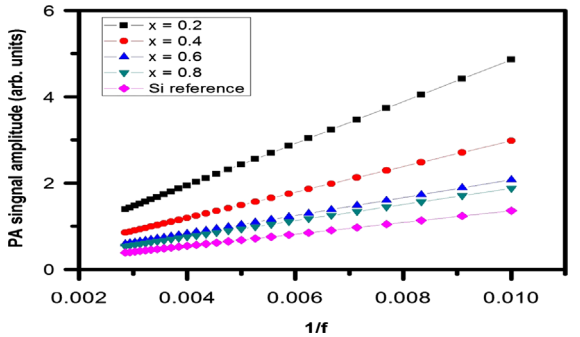

Fig. 5. PA signal amplitude versus f^{-1} for alloyed $CdTe_xS_{1-x}$ NCs and Si reference.

The corresponding values of thermal conductivity k $(=e\sqrt{\alpha})$ [1,31] are also displayed in Table 2.

From the Table 2, it can be seen that when the value of x increases, the values of α, e and k increase. These values are about one order of magnitude larger than that for the bulk values of CdTe [28,32] and CdS [28]. Such an increase in the diffusivity and conductivity are in reasonable agreement with the results of other authors [33]. In their work they obtained values of the $\alpha=1.7\times10^{-5}$ m^2/s and $k=50.16$ W/m/K in the case of ZnO nanoparticles that are larger by one order of magnitude than the bulk value. The increase in α of NCs compared to the bulk because at this small size, quantum confinement is achieved and the interface will form extremely dense network paths for fast diffusion through the NCs. The significant increases of alloyed $CdTe_xS_{1-x}$ thermo physical properties by adding a small amount of Te were predicted. The presence of a phase with high thermal conductivity, which results in increase of the heat flow leads to an increase in the thermo physical properties of the alloyed NCs sample.

4. Conclusions

Photoacoustic (PA) technique has been used to study the optical and thermal properties for alloyed $CdTe_xS_{1-x}$ nanocrystals (NCs) samples of different molar ratios (x) ($x=0$, 0.2, 0.4, 0.5, 0.6 0.8, and 1). Alloyed NCs were synthesized using chemical deposition method. The PA spectra shifted to lower energy region with increasing x. The PA spectra were compared with regular UV–Vis absorption which gives comparable results. The use of Vegard′s law to determine the alloyed NCs parameters is fundamental to get the alloyed NCs size. That is close agreement with the measured values as measured by HRTEM. Furthermore, PA technique is able to determine the thermal parameters (α, e, k) of the same samples. The values of thermal conductivity and diffusivity are one order of magnitude larger than that of bulk values.

Acknowledgements

The authors wish to thank Taif University for the grant research No. (1/433/1865). Quantum Optics Research

Group (QORG) at Deanship of Scientific Research—Taif University is also thanked for their assistance during this work.

References

[1] N. Al-Hosiny, A. Badawi, M.A.A. Moussa, R. El-Agmy, S. Abdallah, Int. J. Nanopart 5 (2012) 258–266.
[2] S. Baskoutas, A.F. Terzis, Mater. Sci. Eng., B 147 (2008) 280–283.
[3] J. Jiao, Z.-J. Zhou, W.-H. Zhou, S.-X. Wu, Mater. Sci. Semicond. Process 16 (2013) 435–440.
[4] A. Badawi, N. Al-Hosiny, S. Abdallah, S. Negm, H. Talaat, Sol. Energy 88 (2013) 137–143.
[5] Y. Wang, Y. Hou, A. Tang, B. Feng, Y. Li, J. Liu, et al., J. Cryst. Growth 308 (2007) 19–25.
[6] R.E. Bailey, S. Nie, J. Am. Chem. Soc 125 (2003) 7100–7106.
[7] N.P. Gurusinghe, N.N. Hewa-Kasakarage, M. Zamkov, J. Phys. Chem. C 112 (2008) 12795–12800.
[8] L.A. Swafford, L.A. Weigand, M.J.B. II, J.R. McBride, J.L. Rapaport, T.L. Watt, et al., J. Am. Chem. Soc. 128 (2006) 12299–12306.
[9] P.K. Khanna, N. Singh, J. Lumin. 127 (2007) 474–482.
[10] C.-W. Peng, Y. Li, J. Nanomater (2010). (Article ID 676839:11).
[11] P.V. Kamat, J. Phys. Chem. C 112 (2008) 18737–18753.
[12] A. Badawi, N. Al-Hosiny, S. Abdallah, S. Negm, H. Talaat, J. Mater. Sci. Eng., A 1 (2011) 942–947.
[13] S. Abdallah, N. Al-Hosiny, A. Badawi, J. Nanomater 2012 (2012) 6.
[14] S. Abdallah, T.A. El-Brolossy, S. Negm, H. Talaat, Eur. Phys. J. Spec. Top. 153 (2008) 199–202.
[15] A. Badawi, N. Al-Hosiny, S. Abdallah, S. Negm, H. Talaat, J. Mater. Sci. Eng., A 2 (2012) 1–6.
[16] A. Rosencwaig, A. Gersho, J. Appl. Phys. 47 (1976) 65–69.
[17] P. Raji, K. Ramachandran, C. Sanjeeviraja, J. Mater. Sci. 41 (2006) 5907–5914.
[18] C.K. Sheng, W.M.M. Yunus, W.M.Z.W. Yunus, Z.A. Talib, A. Kassim, Physica B 403 (2008) 2634–2638.
[19] A.M. Okasha, M. B.Mohamed, T. Abdallah, A.B. Basily, S. Negm, H. Talaat, J. Phys. Conf. Ser. 214 (2010) 012131.
[20] T. Toyoda, T. Hayakawa, Q. Shen, Mater. Sci. Eng., B 78 (2000) 84–89.
[21] D.V. Talapin, S. Haubold, A.L. Rogach, A. Kornowski, M. Haase, H.A. Weller, J. Phys. Chem. B 105 (2001) 2260–2263.
[22] Y.-K. Kuo, B-T. Liou, S.-H. Yen, H.-Y. Chu, Opt. Commun. 237 (2004) 363–369.
[23] M.F. Kotkata, A.E. Masoud, M.B. Mohamed, E.A. Mahmoud, Physica E 41 (2009) 1457–1465.
[24] B. Pejova, A. Tanuševski, I. Grozdanov, J. Solid State Chem. 177 (2004) 4785–4799.
[25] A. Badawi, N. Al-Hosiny, S. Abdallah, H. Talaat, Mater. Sci. Poland 31 (2013) 6–13.
[26] N.M. Al-Hosiny, S. Abdallah, M.A.A. Moussa, A. Badawi, J. Polym. Res. 20 (2013) 1–8.
[27] S. Kolahi, S. Farjami-Shayesteh, Y. Azizian-Kalandaragh, Mater. Sci. Semicond. Process. 14 (2011) 294–301.
[28] O. Madelung, Semiconductors: Data Handbook, third ed. Springer-Verlag, Berlin, 2004.
[29] P. Raji, C. Sanjeeviraja, K. Ramachandran, Cryst. Res. Technol 39 (2004) 617–622.
[30] A. Abdelalim, S. Abdallah, K. Easawi, S. Negm, H. Talaat, J. Phys. Conf. Ser. 214 (2010) 012136.
[31] T.A. El-Brolossy, S.S. Ibrahim, Thermochim. Acta 509 (2010) 46–49.
[32] S. Adachi, Handbook on Physical Properties of Semiconductors, vol. 1–3, Springer-Verlag, 2004, 333.
[33] P.V.B. Lakshmi, K. Ramachandran, Int. J. Thermophys. 28 (2007) 1353–1370.